Journal of Industrial and Engineering Chemistry 17 (2011) 651–656

Contents lists available at ScienceDirect

Journal of Industrial and Engineering Chemistry

journal homepage: www.elsevier.com/locate/jiec

Study on the ClO_4 doped PEDOT-PEG in organic solvent using a hole injection layer for PLEDs

In-Sung Song, Soo-Won Heo, Jang-yong Lee, Doo-Kyung Moon [*]

Department of Materials Chemistry and Engineering, Konkuk University, 1 Hwayang-dong, Gwangjin-gu, Seoul 143-701, Republic of Korea

ARTICLE INFO

Article history:
Received 18 May 2010
Accepted 13 July 2010
Available online 19 February 2011

Keywords:
Polymer light emitting diodes (PLEDs)
Indium tin oxide (ITO)
PEDOT:PSS
Perchlorate doped poly(3,4-ethylenedioxythiophene)-co-poly(ethyleneglycol) (perchlorate doped PEDOT-PEG
Aedotron^{TM} C)

ABSTRACT

Perchlorate doped poly(3,4-ehylenedioxythiophene)-co-poly(ethyleneglycol) (PEDOT-PEG, Aedotron^{TM} C) was introduced as a hole injection layer in PLEDs. Aedotron^{TM} C layer, conductivity and PH were 0.1–2.0 S/cm and ~6.0, respectively, was laid between ITO and PEDOT:PSS. This layer prevented corrosion of the ITO transparent electrode by PSS and acted as an efficient electron blocking layer. Consequently, maximum brightness was increased to about 59% and the stability of the device was improved.

1. Introduction

Owing to their solubility in organic solvents, π-conjugated polymers are receiving considerable attention as materials for next-generation devices such as organic photovoltaic (OPV) cells, organic thin film transistors (OTFT), and organic light emitting devices (OLED), with numerous studies being conducted to explore their physical properties and practical applications [1–7]. In particular, OLEDs formed through an evaporation process using small molecules for the emitting layer have been widely commercialized in small displays, cell phones, etc. While enjoying an advantage over LCDs in allowing a more differentiated range of products, the evaporation process used in their manufacture poses certain limitations to further development. By contrast, OLEDs that use π-conjugated polymers for the emitting layer (i.e., polymer light emitting diodes, PLEDs), thus employs a soluble process, and offer advantages such as low manufacturing costs, a simpler manufacturing process, and the possibility of creating flexible, large-area displays. They do, however, fall short on efficiency, and many studies are being conducted to overcome this drawback. In a PLED, electrons are injected from the cathode and holes are injected from the anode. The electrons and holes recombine in the emitting polymers and then exit before returning to a ground state and emitting light in the process. Thus, the effective injection of electrons and holes are essential for enhancing efficiency [8–10]. To this end, research is currently underway to improve device properties: by applying surface treatment to the anode [11–13] using a cathode material with a low work function [14], adopting an injecting/transporting layer for electrons or holes, and introducing modifications to the electrodes [15–21].

Poly(3,4-ethylenedioxythiophene) blended with poly(styrene-sulfonate) (PEDOT:PSS) is one of the most widely used materials for the hole transport layer in PLEDs. It reduces the surface roughness of indium tin oxide (ITO), facilitates the injection of holes into the emitting layer by adjusting the work function, and prevents the oxidation of light emitting materials when they interface with the emitting layer. However, the PSS in PEDOT:PSS is a strong acidic functional group; it causes corrosion of ITO and diffusion of indium into the emitting layer [22,23]. To redress this problem, researchers improved device performance by developing triphenyldiamine (TPD) [24] and triphenylamine (TPA) [25] with cross-linkable trifluorovinyl ether (TFV), and made it possible to fabricate multi-layered PLEDs. A broad range of hole injection/transportation materials have also been developed, but the need for a multi-step combination process tends to compromise their effectiveness.

Therefore, the current study fabricated a PLED with a novel structure by introducing a hole injection layer (HIL) consisting of perchlorate doped poly(3,4-ehylene dioxythiophene)-co-poly(ethylene-glycol) (PEDOT-PEG, Aedotron^{TM} C) (Fig. 1), which is neutral

---

[*] Corresponding author. Tel.: +82 2 450 3498; fax: +82 2 444 0765.
E-mail address: dkmoon@konkuk.ac.kr (D.-K. Moon).

1226-086X/$ – see front matter © 2011 The Korean Society of Industrial and Engineering Chemistry. Published by Elsevier B.V. All rights reserved.
doi:10.1016/j.jiec.2011.02.005

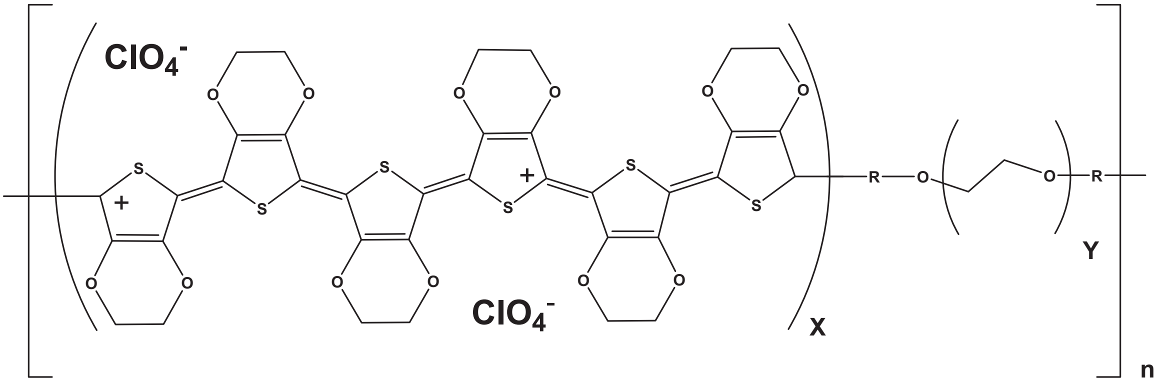

Fig. 1. Molecule structures of Aedotron™ C.

and has high conductivity. UV–visible spectroscopy was used to evaluate the transmittance and solvent resistance of an Aedotron™ C thin film, and an atomic force microscope was used to observe the surface morphology of film. Finally, the structure of the fabricated device was optimized via characterization using an I–V–L test according to the thickness and thermal treatment temperature of the Aedotron™ C and the thickness of the PEDOT:PSS.

2. Experimental

2.1. Materials

Orange color polymer was used for the emitting layer. The perchlorate doped poly(3,4-ehylenedioxythiophene)-co-poly(ethylene-glycol) (PEDOT-PEG, Aedotron™ C) was purchased from Aldrich, while the poly(3,4-ethylenedioxythiophene) blended with poly(styrenesulfonate) (PEDOT:PSS, AI4083) was purchased from Baytron.

2.2. Measurements

All thin films were manufactured using a GMC2 spin coater (Gensys), and their thickness was measured using an alpha step 500 surface profiler (KLA-Tencor). The absorbance of the Aedotron™ C film was measured using an Agilent 8453 UV–visible spectrometer (HP Agilent), and the transmittance and conductivity was measured with a 4-point probe station (MST6000C). Also, the electro-optical properties of the fabricated device were characterized using a Keithley 2400 source meter unit (Keithley) and a PR 670 spectra scan (Photo Research), while the surface morphology of thin film was measured using an atomic force microscope (AFM, PSIA XE-150).

2.3. ITO cleaning and film formation of Aedotron™ C

To clean the ITO glass (10 Ω/sq, Samsung Corning), sonication was performed using detergent (Alconox® in deionized water, 10%), acetone, IPA (isopropylalcohol), and deionized water, in the order listed, for 20 min respectively. Moisture was blown thoroughly with N_2 gas. In order to ensure the complete removal of all remaining water, the ITO was baked on a hot plate for 10 min at 120 °C. To administer hydrophilic treatment to the glass surface, it was cleaned for 10 min in a UVO cleaner. For measurement of the solvent resistance of the Aedotron™ C film, Aedotron™ C filtered with a 5 μm PTFE syringe filter was used to coat the cleaned ITO glass at a speed of 3000 rpm, resulting in a thin film with a thickness of 45 nm. This thin film was annealed for 20 min at 140 °C, and then rinsed using DI water, chlorobenzene, chloroform, and methyl chloride. To measure the thickness and transmittance of the thin film relative to the spin coating speed of Aedotron™ C, spin coating was performed at a speed varying from 500 to 5000 rpm. The film was then annealed for 20 min at 140 °C, before its thickness and transmittance were measured. Also, a 4-point probe station was used to gauge the conductivity of PEDOT:PSS and Aedotron™ C.

2.4. Fabrication of PLEDs

The PEDOT:PSS and Aedotron™ C were filtered using a 0.45 μm PTFE syringe filter and a 5 μm PTFE syringe filter, and then shaken for 24 h. The orange color polymer for the emitting layer was dissolved in chlorobenzene (solution of 0.5 wt%) and shaken for 24 h, before being filtered using a 5 μm PTFE syringe filter. To create the device, the patterned ITO glass, cleaned as described above, was spin coated with Aedotron™ C to a thickness of 35–130 nm and annealed at temperatures ranging from 100 to 180 °C. The PEDOT:PSS was applied via spin coating to a thickness of 35–55 nm, and then subjected to annealing for 20 min at PEDOT:PSS. The orange color polymer coating was applied to a thickness of 80 nm, and then annealed for 1 h at 90 °C to remove all residual solvents. The metal electrode was subjected to thermal deposition in a high vacuum chamber (1×10^{-6} Torr or below) using BaF_2 (0.1 Å/s, 2 nm), Ba (0.2 Å/s, 2 nm), and Al (5 Å/s, 200 nm), in the order listed. To protect the organic layer and the electrode layer from H_2O and O_2, a getter was attached to the inside of the glass cover to encapsulate the device. The composition of the fabricated device is shown in Fig. 2.

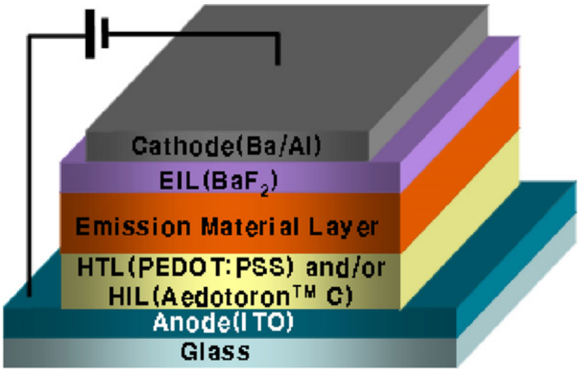

Fig. 2. Structure of PLEDs in this study.

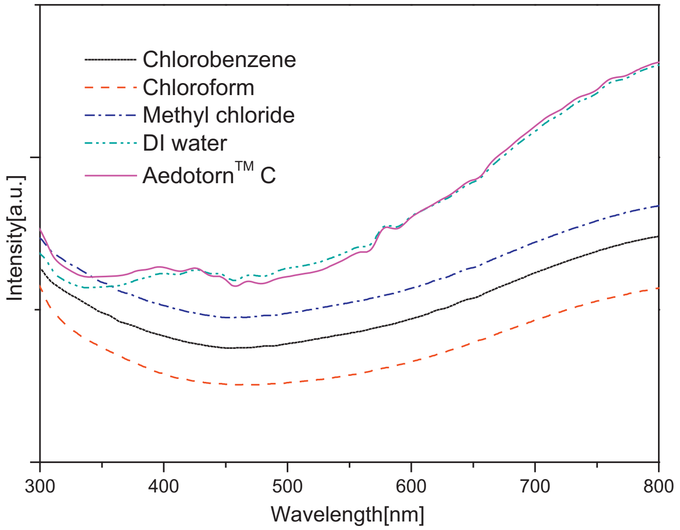

Fig. 3. Absorption spectrums of before/after solvents.

3. Results and discussion

3.1. Thin film of Aedotron™ C

The absorbance of the Aedotron™ C thin film did not change significantly after rinsing with DI water (Fig. 3), but changed dramatically after rinsing with chlorobenzene, methyl chloride, and chloroform. This shows that the Aedotron™ C thin film was dissolved by these organic solvents. Because Aedotron™ C takes the form of ClO_4^- doped with PEDOT and poly(ethylene glycol) (PEG) and dispersed in nitromethane (CH_3NO_2), it exhibits weak solvent resistance to the organic solvents listed above. Therefore, in the case of polymer thin films formed by dissolving in organic solvents, it can be predicted that surface mixing will occur when a polymer layer is applied to an Aedotron™ C thin film through spin coating.

Fig. 4 shows the measured thickness of the thin films after spin coating with Aedotron™ C at a speed ranging from 500 to 5000 rpm. As the spin coating speed decreased, the thickness of the thin film increased quadratically. At speed exceeding 2000 rpm, it was possible to obtain thin films possessing a relatively consistent thickness, with a uniformity of ±5 nm. However, at 500 and 1000 rpm, the thickness of the thin film showed a uniformity of ±10 nm.

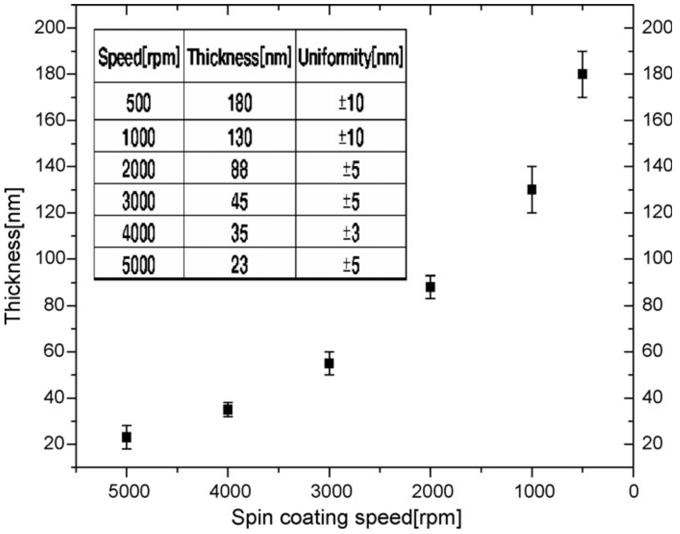

Speed[rpm]	Thickness[nm]	Uniformity[nm]
500	180	±10
1000	130	±10
2000	88	±5
3000	45	±5
4000	35	±3
5000	23	±5

Fig. 4. Thickness of Aedotron™ C thin films by spin coating speed.

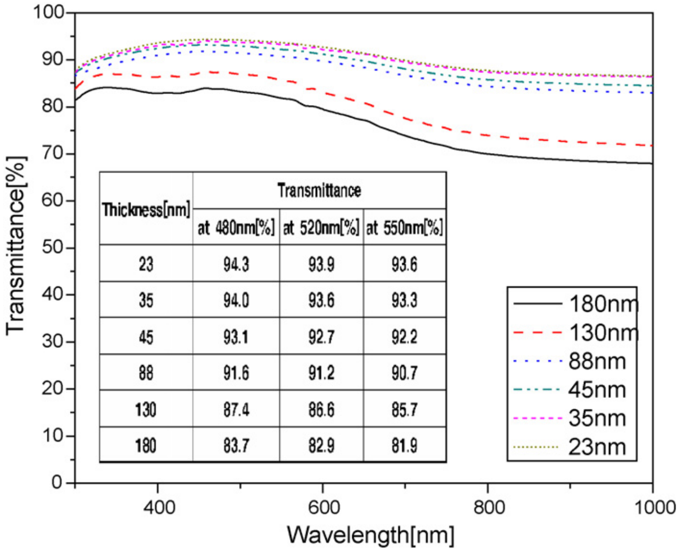

Thickness[nm]	Transmittance		
	at 480nm[%]	at 520nm[%]	at 550nm[%]
23	94.3	93.9	93.6
35	94.0	93.6	93.3
45	93.1	92.7	92.2
88	91.6	91.2	90.7
130	87.4	86.6	85.7
180	83.7	82.9	81.9

Fig. 5. Transmittance of Aedotron™ C by thickness.

Fig. 5 shows the measured transmittance of the thin films relative to thickness using UV–visible spectroscopy. When the thickness was 180 nm and 130 nm, the transmittance was low at 81.9% and 85.7% (at 550 nm, visible region), respectively. By contrast, the transmittance increased to 90% or higher at a thickness of 88 nm or less. At around 23 nm, in particular, a high transmittance of 93.6% could be observed. Since this is higher than the transmittance of PEDOT:PSS, which ranges between 80 and 90%, it can be predicted that applying Aedotron™ C thin films as an interlayer will reduce optical absorption and light scattering in the emitting layer.

3.2. Characterization of PLEDs

Fig. 2 shows the structure of the PLED device created in this study. The brightness-voltage and efficiency-current density of Device IV relative to Aedotron™ C thickness and thermal treatment temperature are shown in Figs. 6 and 7, respectively. Turn-on voltage was found to be 2 V in all cases regardless of the

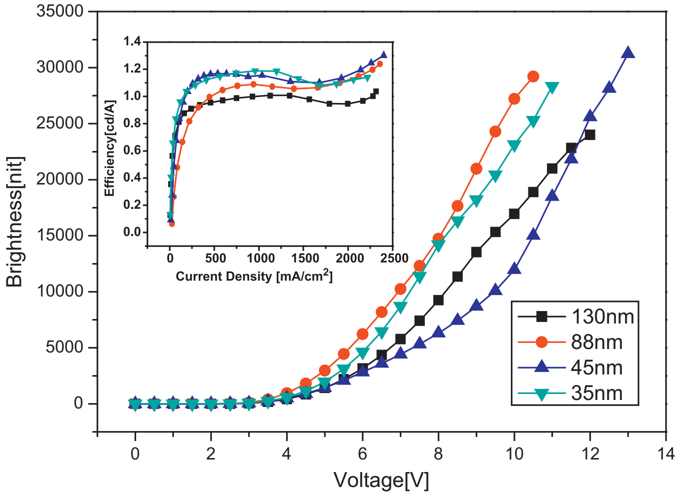

Fig. 6. Brightness-voltage and efficiency-current density graph (inset) by various thicknesses of Aedotron™ C (Device configuration: ITO/Aedotron™ C (35–130 nm)/PEDOT:PSS (40 nm)/Polymer (80 nm)/BaF_2 (2 nm)/Ba (2 nm)/Al (200 nm)).

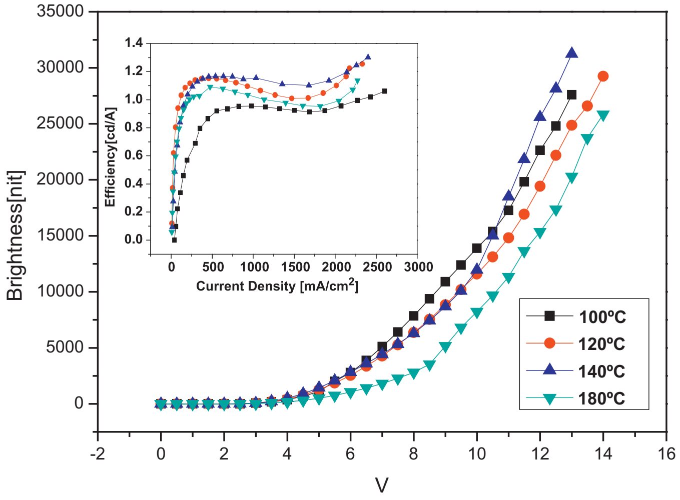

Fig. 7. Brightness-voltage and efficiency-current density graph (inset) by various annealing temperatures of Aedotron^{TM} C (Device configuration:ITO/Aedotron^{TM} C (45 nm)/PEDOT:PSS (40 nm)/Polymer (80 nm)/BaF_2 (2 nm)/Ba (2 nm)/Al (200 nm)).

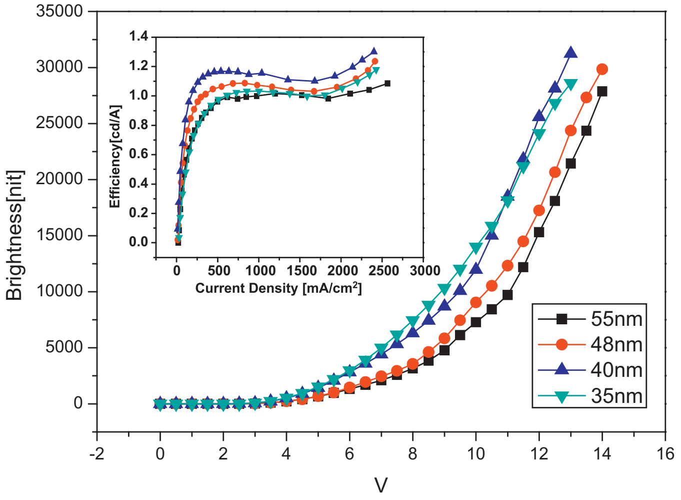

Fig. 8. Brightness-voltage and efficiency-current density graph (inset) by various thicknesses of PEDOT:PSS (Device configuration:ITO/Aedotron^{TM} C (45 nm)/PEDOT:PSS (35–55 nm)/Polymer (80 nm)/BaF_2 (2 nm)/Ba (2 nm)/Al (200 nm)).

Aedotron^{TM} C thickness and thermal treatment temperature. The device exhibited the most desirable properties when Aedotron^{TM} C was applied to a thickness of 45 nm and thermal treatment was performed at 140 °C.

The brightness-voltage and efficiency-current density of Device IV relative to PEDOT:PSS thickness are shown in Fig. 8. The turn-on voltage remained unchanged at 2 V, and the device with a PEDOT:PSS thickness of 40 nm showed the most desirable properties.

Fig. 9 shows the brightness-voltage and efficiency-current density graph for Devices I through IV. The structures and conditions of fabrication for each are summarized in Table 1. In the case of Device I, which uses PEDOT:PSS as the hole transport layer (HTL), the maximum brightness was 19,585 cd/m^2. By contrast, Device IV, which used Aedotron^{TM} C for the hole injection layer (HIL) and had an Aedotron^{TM} C/PEDOT:PSS structure, the maximum brightness was increased by roughly 59% to 31,231 cd/m^2. Maximum efficiency remained unchanged at 1.30 cd/A with or without Aedotron^{TM} C.

Fig. 10 shows the EL spectrum. Device IV had an FWHM (full width at half maximum) of 106 nm, thus exhibiting superior color purity to Device I, which had an FWHM of 118 nm.

Device II had a maximum brightness and maximum efficiency of 4627 cd/m^2 and 0.28 cd/A, respectively, and Device III had a maximum brightness and maximum efficiency of 5108 cd/m^2 and 0.27 cd/A, respectively. In both cases, the measurements were far lower than those for Device I, the maximum brightness and maximum efficiency of which were 19,585 cd/m^2 and 1.30 cd/A. This can be explained by surface mixing and analysis of the thin film's surface morphology. After the Aedotron^{TM} C thin film was rinsed with organic solvents, its surface was observed to have transformed due to a change in UV absorbance (Fig. 3). The reason lies in the properties of the Aedotron^{TM} C dispersed in the organic solvents. If a polymer dissolved in an organic solvent such as chlorobenzene is coated over Aedotron^{TM} C, interface mixing occurs between the two layers, making hole injection difficult. This, in turn, reduces the generation of exitons, which decreases both the maximum brightness and maximum efficiency. In addition, observation of the surface morphology of Devices II and III through an AFM (Fig. 11(c)) revealed that the roughness of the Aedotron^{TM} C thin film hindered the movement of holes at the interface.

On the other hand, Device IV showed a maximum brightness of 31,231 cd/m^2 and a maximum efficiency of 1.30 cd/A, reflecting a 59% enhancement in maximum brightness over Device I, which did not use Aedotron^{TM} C. This can be attributed to the introduction of Aedotron^{TM} C, which is neutral (pH: −6.0), between the ITO layer and the PEDOT:PSS layer, which prevented the corrosion of ITO by acid and caused the maximum brightness to increase. Because Aedotron^{TM} C has strong solvent resistance to DI water (Fig. 3), interface mixing with the PEDOT:PSS layer did not occur. One disadvantage is that the root mean square (RMS) of the Aedotron^{TM} C as observed through the AFM is relatively large at 42.39 nm. However, in the case of Device IV, with PEDOT:PSS coated over Aedotron^{TM} C, the PEDOT:PSS served to fill in the rough surface of the Aedotron^{TM} C, thereby producing a smoother surface plane and thus reducing the RMS to 35.79 nm. In spite of it, the reason why the properties of Device IV was improved more than Device I is due to the difference of conductivity of PEDOT:PSS and Aedotron^{TM} C. In the structure of Device IV, the conductivity of Aedotron^{TM} C is

Table 1
Characteristics of devices.

Structures		Turn on voltage [V]	Max brightness [cd/m^2]	Max efficiency [cd/A]	CIE coordinates	λ_{max} [nm]	Full width at half maximum [FWHM, nm]
I	PEDOT:PSS (40 nm)		19585	1.30	(0.57, 0.42)	586	118
II	Aedotron^{TM} C (45 nm)	2.5	4627	0.2873	(0.54, 0.45)	588	120
III	PEDOT:PSS (40 nm)/Aedotron^{TM} C (45 nm)	2.5	5108	0.2782	(0.57, 0.42)	590	118
IV	Aedotron^{TM} C (35–130 nm)/PEDOT:PSS (35–55 nm)	2.0	31231	1.30	(0.57, 0.42)	582	106

ITO (170 nm)/I–IV/orange polymer (80 nm)/BaF_2 (2 nm)/Ba (2 nm)/Al (200 nm).

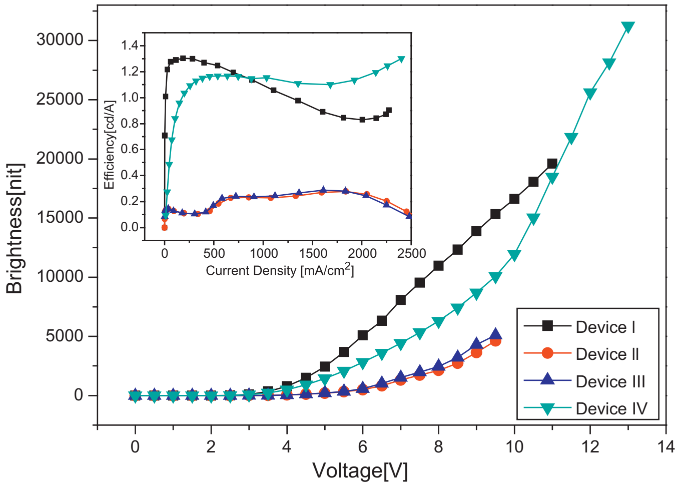

Fig. 9. Brightness-voltage and efficiency-current density graph (inset) of devices.

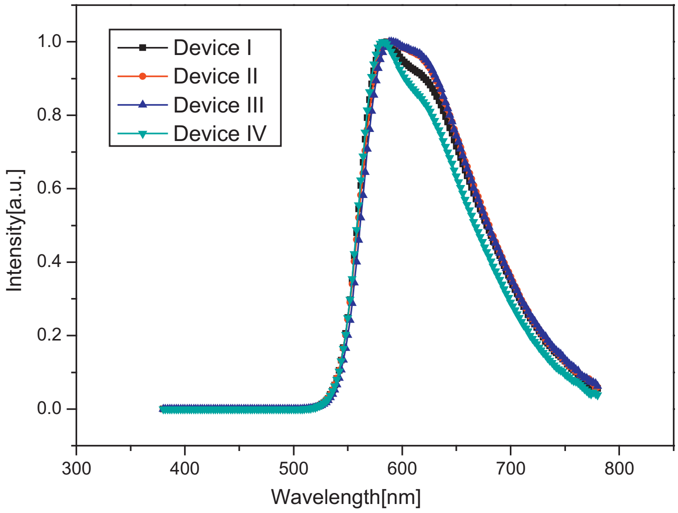

Fig. 10. EL spectrum of devices.

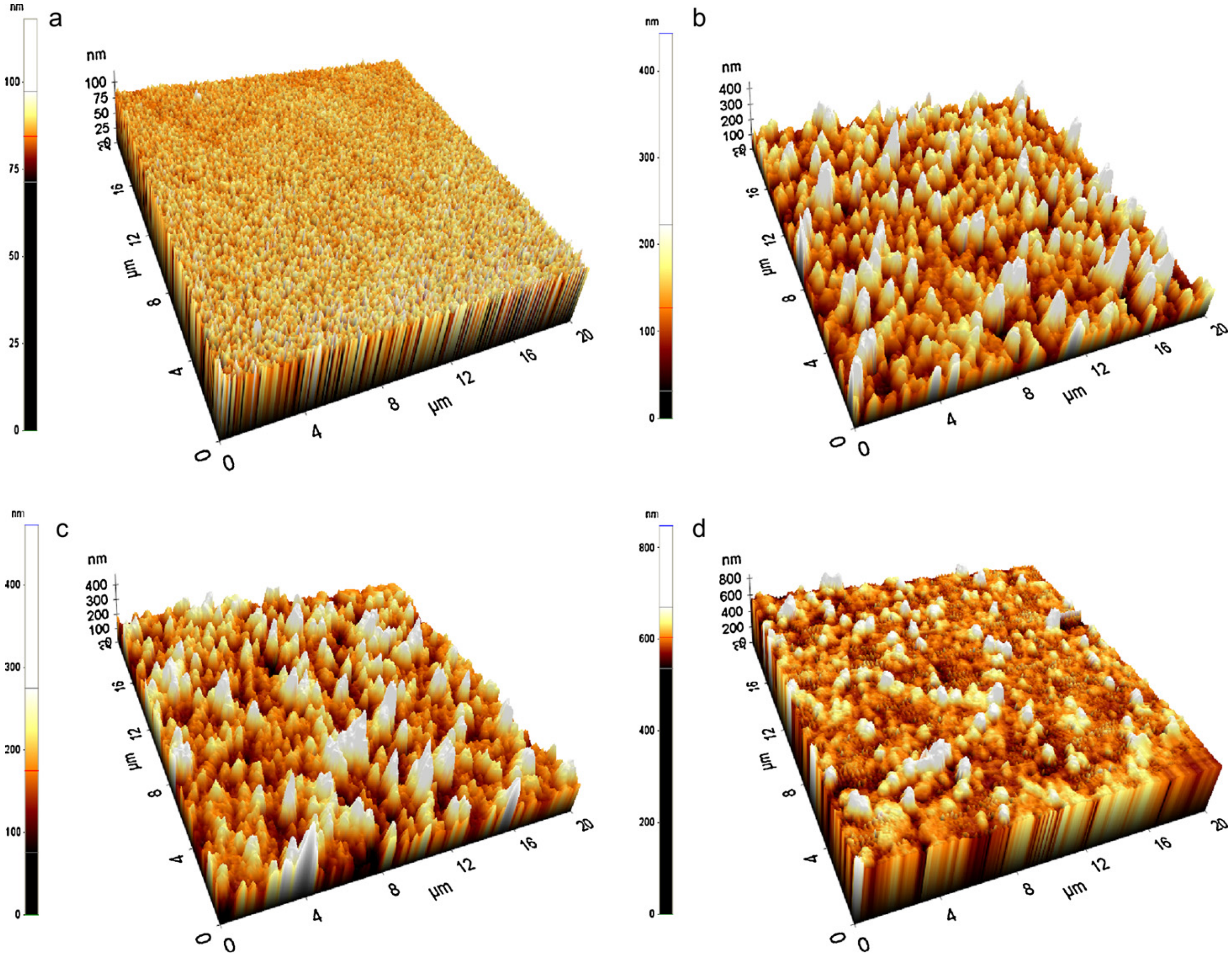

Fig. 11. AFM images of devices (I–IV). (a) Surface morphology of ITO/PEDOT:PSS (RMS:3.13 nm). (b) Surface morphology of ITO/Aedotron^{TM}C (RMS:42.39 nm). (c) Surface morphology of ITO/PEDOT:PSS/Aedotron^{TM}C (RMS:52.12 nm). (d) Surface morphology of ITO/Aedotron^{TM}C/PEDOT:PSS (RMS:35.79 nm).

0.1–2 S/cm, which is much higher than PEDOT:PSS with 10^{-3}–10^{-4} S/cm. To improve the EL properties of PLEDs, the injection balance of hole and electron is significantly important. Therefore, the injection property of hole from anode was improved by applying Aedotron^{TM} C, which has good conductivity, as an HIL. As a result, Device IV, which Aedotron^{TM} C was applied, enhanced maximum brightness up to about 59% than Device I.

Also, as seen in the inset in Fig. 9, Device I exhibited good efficiency in sections with a current density of 750 mA/cm^2 or below. But as the current density increased beyond this level, the efficiency of Device IV actually surpassed that of Device I, thus showing that Device IV has superior device stability without degradation at high current densities.

4. Conclusion

In this study, a new HIL/HTL structure which uses Aedotron^{TM} C, a neutral material, as a buffer layer between ITO and PEDOT:PSS was developed. It was thus possible to enhance the maximum brightness and stability of the fabricated device while preventing the corrosion of ITO by PSS, which is a strong acid. Although the Aedotron^{TM} C thin film showed damage from organic solvents such as chlorobenzene, chloroform, and methyl chloride, it exhibited strong solvent resistance against DI water, making it suitable for application as an interlayer between the ITO anode and the PEDOT:PSS layers. In addition, Aedotron^{TM} C, which has a conductivity of 0.1–2 S/cm, facilitated the transport of holes from the anode to the emitting layer. By applying a layer of Aedotron^{TM} C, the maximum brightness of the fabricated device could be increased by 59% without incurring a reduction in maximum efficiency. Color purity was also enhanced, with an FWHM of 106 nm, and degradation of the device did not occur even when the applied voltage was increased. It was thus confirmed that the device using Aedotron^{TM} C was substantially more stable than that using only PEDOT:PSS.

References

[1] S.H. Jin, H.J. Park, J.Y. Kim, K. Lee, S.P. Lee, D.K. Moon, H.J. Lee, Y.S. Gal, Macromolecules 35 (2002) 7532–7534.
[2] J.Y. Lee, Y.J. Kwon, J.W. Woo, D.K. Moon, Journal of Industrial and Engineering Chemistry 14 (2008) 810.
[3] J.Y. Lee, W.S. Shin, J.R. Haw, D.K. Moon, Journal of Materials Chemistry 19 (2009) 4938.
[4] J.H. Burroughes, D.D.C. Bradley, A.R. Brown, R.N. Marks, K. Mackey, R.H. Friend, P.L. Burns, A.B. Holmes, Nature 347 (1990) 539.
[5] R.H. Friend, R.W. Gymer, A.B. Holmes, J.H. Burroughes, D.D.C. Bradley, D.A.D. Santos, J.L. Bredas, M. Loglund, W.R. Salaneck, Nature 397 (1999) 121.
[6] J.S. Lee, J.S. Suh, I.H. Cho, Journal of Industrial and Engineering Chemistry 7 (6) (2001) 396.
[7] K.S. Yook, J.Y. Lee, Journal of Industrial and Engineering Chemistry 16 (2010) 181.
[8] F. Garten, A. Hilberer, F. Cacialli, E. Esselink, Y.V. Dam, B. Schlatmann, R.H. Friend, T.M. Klapwijk, G. Hadziioannou, Advanced Materials 9 (2) (1997) 127.
[9] Y.Z. Lee, X. Chen, S.A. Chen, P.K. Wei, W.S Fann, Journal of the American Chemistry Society 123 (10) (2001) 2296.
[10] D. Liu, F. Teng, Z. Xu, S. Yang, L. Qian, Q. He, Y. Wang, X. Xu, Journal of Luminescence 122–123 (2007) 656.
[11] J.S. Kim, R.H. Friend, F. Cacialli, Applied Physics Letters 74 (21) (1999) 3084.
[12] Q. Huang, G. Evmenenko, P. Dutta, P. Lee, N.R. Armstrong, T.J. Marks, Journal of the American Chemistry Society 127 (29) (2005) 10227.
[13] S. Kato, Journal of the American Chemistry Society 127 (2005) 11538.
[14] H. Wu, F. Huang, Y. Mo, W. Yang, D. Wang, J. Peng, Y. Cao, Advanced Materials 16 (20) (2004) 1826.
[15] S.H. Oh, D. Vak, S.I Na, Advanced Materials 20 (9) (2008) 1624.
[16] F. Huang, Y.-H. Niu, Y. Zhang, J.-W. Ka, M.S. Liu, A.K-Y. Jen, Advanced Materials 19 (2007) 2010.
[17] T.W. Lee, H.C. Lee, O.O. Park, Applied Physics Letters 81 (2) (2002) 214.
[18] T.F. Guo, F.S. Yang, Z.J. Tsai, T.C. Wen, S.N. Hsieh, Y.S. Fu, Applied Physics Letters 87 (1) (2005) 013504.
[19] X.Y. Deng, W.M. Lau, K.Y. Wong, K.H. Low, H.F. Chow, Y. Cao, Applied Physics Letters 84 (18) (2004) 3522.
[20] J. Cui, Q. Huang, Q. Wang, T.J. Marks, Langmuir: the ACS Journal of Surfaces and Colloids 17 (7) (2001) 2051.
[21] J. Lee, B.-J.. Jung, J.-I.. Lee, H.K. Shim, Journal of Materials Chemistry 12 (12) (2002) 3494.
[22] W.H. Kim, A. Makinen, N. Nikolov, Applied Physics Letters 80 (20) (2002) 3844.
[23] M.P. de Jong, L.J. van IJzendoorn, M.J.A. de Voigt, Applied Physics Letters 77 (14) (2000) 2255.
[24] Y.H. Niu, Y.L. Tung, Y. Chi, Chemistry of Materials, vol. 17(13), A Publication of the American Chemical Society, 2005,, p. 3532.
[25] B. Lim, J.T. Hwang, J.Y. Kim, J. Ghim, D. Vak, Y.Y. Noh, S.H. Lee, K. Lee, A.J. Heeger, D.Y. Kim, Organic Letters 8 (21) (2006) 4703.